FURIN in insulin receptor processing

Subjects: Biochemistry & Molecular Biology

Contributor: Ilaria Coppola

The insulin receptor (IR) is critically involved in maintaining glucose homeostasis. It undergoes proteolytic cleavage by proprotein convertases, which is an essential step for its activation. The importance of the insulin receptor in the liver is well established, but its role in pancreatic β cells is still controversial.

insulin receptor | proprotein convertase | FURIN | liver | pancreatic β cells | insulin signaling | glucose homeostasis

1. Introduction

The IR is a key regulator of glucose homeostasis. The binding of insulin to its receptor in metabolic organs such as liver, pancreas, muscle, brain, and adipose tissue leads to the activation of a signaling pathway mostly aimed at maintaining glucose homeostasis in humans and animals [1].

The IR is synthesized as an inactive precursor protein (proIR) that needs post-translational modifications to be activated. First, it requires endoproteolytic cleavage at the tetrabasic sequence RKRR^{752}, yielding disulfide-linked α and β subunits [2]. Patients carrying a mutation in this cleavage site present with severe insulin-resistant diabetes [3][4]. The tetrabasic sequence is most likely removed afterward by carboxypeptidase D, a process that has been shown to be required for full activation of the insulin-like growth factor 1 receptor [5]. The endoproteolytic cleavage step has been shown to be performed by the proprotein convertase (PC) family members *FUR*IN, PACE4, PC5/6 (isoforms A and B), and PC7 in overexpression experiments [6]. However, FURIN was put forward as the physiological PC for processing of the proIR in the secretory pathway and PACE4 at the cell surface when FURIN activity is reduced [6]. In colorectal cell lines and in mouse mammary gland tissue, genetic ablation of *Furin* indeed blocked proIR processing, suggesting non-redundant cleavage by FURIN [7][8]. However, the proIR was normally processed in liver of an inducible *Furin* knockout mouse model, revealing tissue-specific redundancy [9]. Cleavage of the proIR by PCs in pancreatic β cells has not been investigated.

Insulin signaling has been studied extensively in many tissues. In liver, it regulates glucose metabolism by suppressing hepatic glucose production and promoting insulin clearance and glycogen storage [10][11]. Liver-specific IR knockout mice show severe glucose intolerance together with hyperinsulinemia, and subsequent hepatic dysfunction [12]. The physiological consequences of reduced IR signaling in β cells remain controversial. Notably, studies in transgenic mice have suggested an important role of the IR in pancreatic β cells for the regulation of peripheral glucose homeostasis [13][14][15]. However, these studies made use of a Cre driver line

shown to have an off-target expression in the brain [16], or were affected by the presence of the human growth hormone (hGH) minigene [17][18][19]. Recent studies, using Cre drivers lacking these pitfalls, showed that in β cells of adult islets, the IR controls insulin release and β-cell physiology [20][21].

2. IR Processing and Signaling Are Severely Affected in *Fur*KO β Cells

To determine the role of FURIN in the proteolytic activation of the proIR in pancreatic β cells, we first analyzed the murine β-cell line βTC3. This cell line showed a similar gene expression pattern of PCs active in the constitutive secretory pathway at mRNA levels compared to mouse islets (Figure 1A). *Furin, Pcsk6,* and *Pcsk7*, encoding FURIN, PACE4, and PC7, respectively, were highly expressed, while *Pcsk5*, encoding PC5/6, was not. In βTC3 cells, the lack of *Furin* (*Fur*KO) resulted in severely impaired, if not blocked, proIR cleavage (Figure 1B), and transfection with recombinant *Furin* rescued the cleavage of mature IR (Figure 1C). Importantly, the uncleaved proIR in *Fur*KO β cells was unable to properly respond to insulin based on lack of phosphorylation of IRS1 and AKT after insulin stimulation (Figure 1D,E).

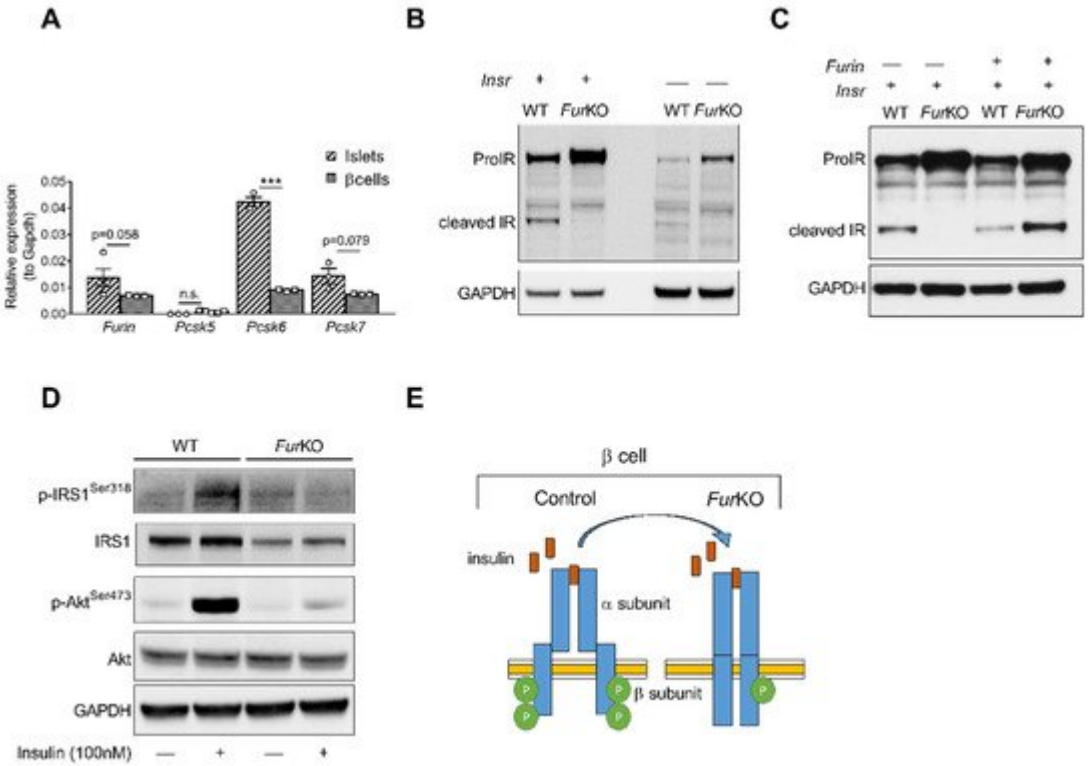

Figure 1. IR processing and signaling are severely affected in *Fur*KO β cells. (**A**) Comparative RT-qPCR analysis of *Furin*, *Pcsk5*, *Pcsk6*, and *Pcsk7* gene expression in the islets of $Fur^{fl/fl}$ mice (n = 3–5 per genotype) and wild-type βTC3 cells. *** $p < 0.001$ determined by two-way ANOVA with Sidak's multiple comparisons test. All the RT-qPCR data were normalized to *Gapdh*. (**B**) Western blot analysis of the IR protein level in the whole-cell lysate of WT and *Fur*KO IR-transfected and non-transfected βTC3 cells. GAPDH was used as loading control. (**C**) Western blot analyses of IR protein levels in whole-cell lysates from βTC3 cells transfected with *Insr* or co-transfected with *Insr*

and *Furin*. GAPDH was used as loading control. (**D**) Western blot analysis of phosphorylated and total IRS1, and Akt in whole-cell lysates from βTC3 cells treated with 100 nM insulin or vehicle for 5 min. GAPDH was used as a loading control. (**E**) Schematic representation of a suggested mechanism of IR signaling in *Fur*KO βTC3 cells compared to a physiological condition.

3. IR Proteolytic Cleavage Is Not Altered in Liver-Specific *Fur*KO Mice

At mRNA level, *Furin* was the most abundant PC in mouse liver, although *Pcsk5* and *Pcsk6* were highly expressed as well (Figure 2A). *In vivo*, conditional knockout of *Furin* in mouse hepatocytes using the Alb-Cre mice (L*Fur*KO; Figure 3A) induced a modest, non-significant increase of *Pcsk5* and *Pcsk6* gene expression (Figure 2A). We subsequently evaluated the IR processing in hepatocytes from L*Fur*KO and control mice by Western blot. As shown in Figure 2B,C, the cleavage of proIR was not significantly reduced in L*Fur*KO mice compared to the controls, indicating almost complete redundancy for proteolytic cleavage by other PCs.

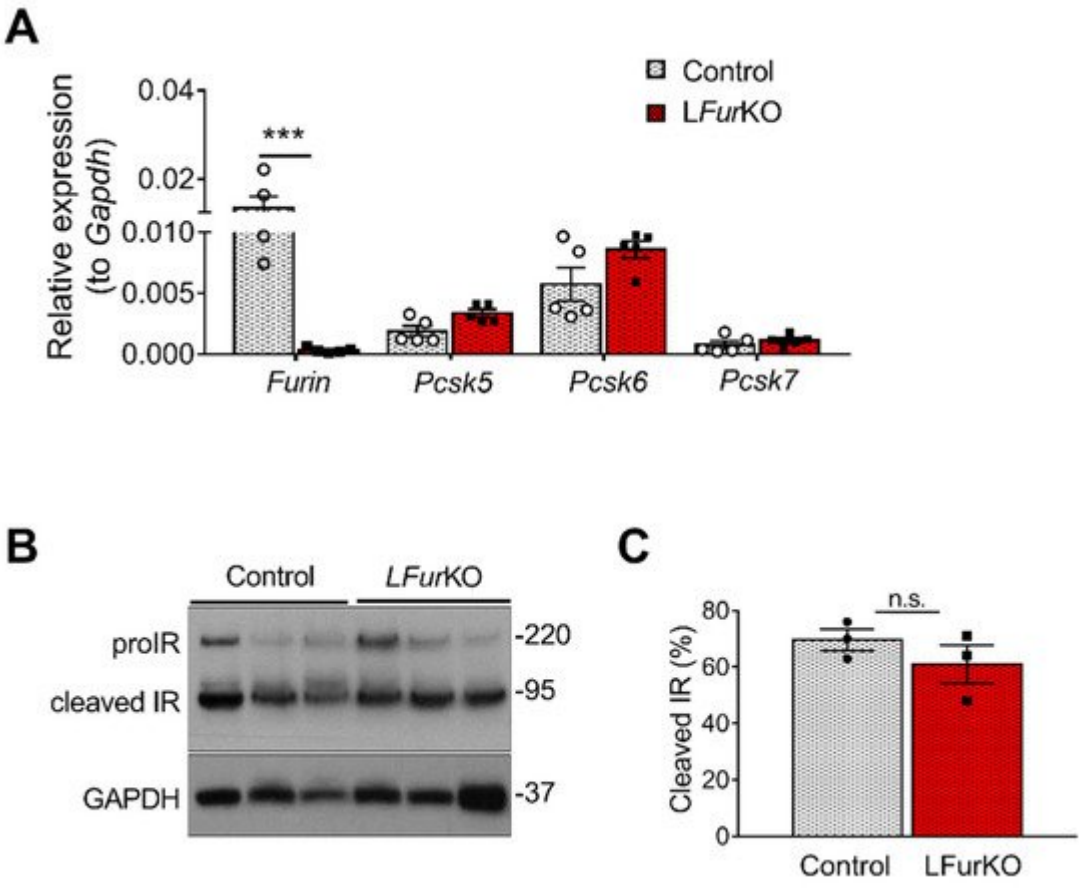

Figure 2. IR proteolytic cleavage is not altered in the liver of *Furin* knockout mice. (**A**) RT-qPCR analysis of *Furin*, *Pcsk5*, *Pcsk6*, and *Pcsk7* gene expression in the liver of either L*Fur*KO or control ($Fur^{fl/fl}$) mice, $n = 5$ per genotype. *** $p < 0.001$ determined by two-way ANOVA with Sidak's multiple comparisons test. All RT-qPCR data were normalized to *Gapdh*. (**B**) Western blot analysis of IR processing from liver membrane fractions of control and L*Fur*KO mice, $n = 3$ animals per genotype. GAPDH was used as a loading control. (**C**) Protein-level quantification

reported as % of cleaved IR over the total IR (ProIR + cleaved IR). ProIR data are represented as the mean ± SEM. Non-significant differences were detected by unpaired *t*-test.

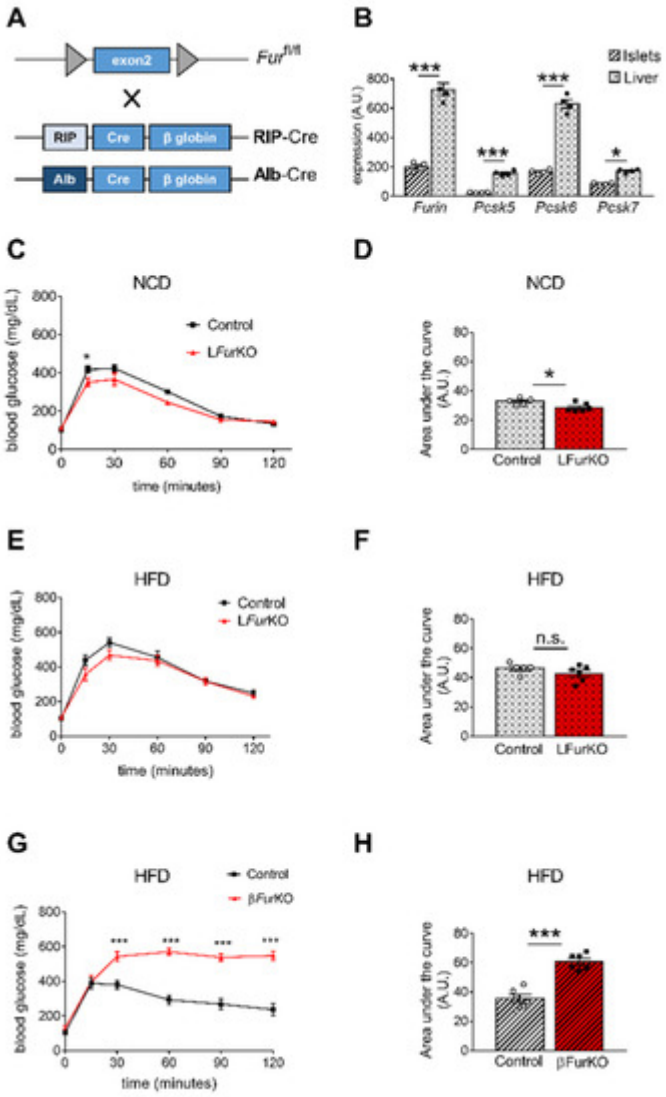

Figure 3. Impact of *Furin* knockout in liver and pancreatic β cells on glucose homeostasis (**A**) Schematic representation of the breeding approach. Mice in which the exon 2 of *Furin* had been floxed (*Fur*$^{fl/fl}$) were crossed with RIP-Cre or Alb-Cre driver lines. (**B**) Microarray analysis of *Furin*, *Pcsk5*, *Pcsk6*, and *Pcsk7* gene expression in liver versus islets of control (*Fur*$^{fl/fl}$) mice, *n* = 4 per genotype. * $p < 0.05$; *** $p < 0.001$ determined by two-way ANOVA with Sidak's multiple comparisons test. All the data were normalized to *Gapdh.* (**C**) Intraperitoneal glucose tolerance tests (IPGTTs) on 8-week-old male L*Fur*KO and control mice on normal chow diet (NCD) (*n* = 5–6 mice/group). * $p < 0.05$ determined by two-way ANOVA with Sidak's multiple comparisons test. (**D**) The area under the curve was expressed as g/dL/120 min; *n* = 5–6 mice/group. * $p < 0.05$ determined by unpaired *t*-test. (**E**) Intraperitoneal glucose tolerance test (IPGTT) on 16-week-old male L*Fur*KO and control (*Fur*$^{fl/fl}$) mice fed for 8 weeks on a high-fat diet (HFD, 45% kJ from fat). No significant differences were found by two-way ANOVA with Sidak's multiple comparisons test. (**F**) The area under the curve was expressed as g/dL/120 min; *n* = 5–6 mice/group. No significant differences were observed by unpaired *t*-test. (**G**) IPGTT on 16-week-old male β*Fur*KO and control (*Fur*$^{fl/fl}$) mice fed for 8 weeks on a HFD (45% kJ from fat). *** $p < 0.001$ determined by two-way ANOVA

with Sidak's multiple comparisons test. (**H**) The area under the curve was expressed as g/dL/120 min; n = 6 mice/group. *** $p < 0.001$ determined by unpaired t-test. All data were presented as mean ± SEM.

4. Impact of Conditional *Furin* Deletion in Liver and Pancreatic β Cells on Glucose Homeostasis

β-cell-specific *Furin* knockout (β*Fur*KO) mice were generated by breeding *Fur*$^{fl/fl}$ mice [9] with RIP-Cre$^{+/-}$ (Figure 3A). A comparative gene expression analysis of all PCs active in the constitutive secretory pathway, *Furin*, *Pcsk5*, *Pcsk6*, and *Pcsk7* in the liver and pancreatic islets of *Fur*$^{fl/fl}$ mice is displayed in Figure 3B and Figure 4. Overall, mRNA expression levels of all tested PCs were significantly higher in mouse liver with respect to isolated mouse islets. We subsequently studied how FURIN deficiency affected glucose homeostasis *in vivo* in both tissue-specific knockout models. As expected, we observed that L*Fur*KO mice remained glucose tolerant both on chow and HFD (Figure 3C–F) with normal insulin sensitivity on HFD (Figure S1B). In contrast, β*Fur*KO mice were severely glucose-intolerant, with significantly higher fasting blood glucose levels on HFD (Figure 3G–H and Figure S1B), even on a chow diet, as we described in a previous study [22]. We also did not observe changes in fasting blood glucose and body weight in L*Fur*KO mice compared to controls (Figure S1C,D).

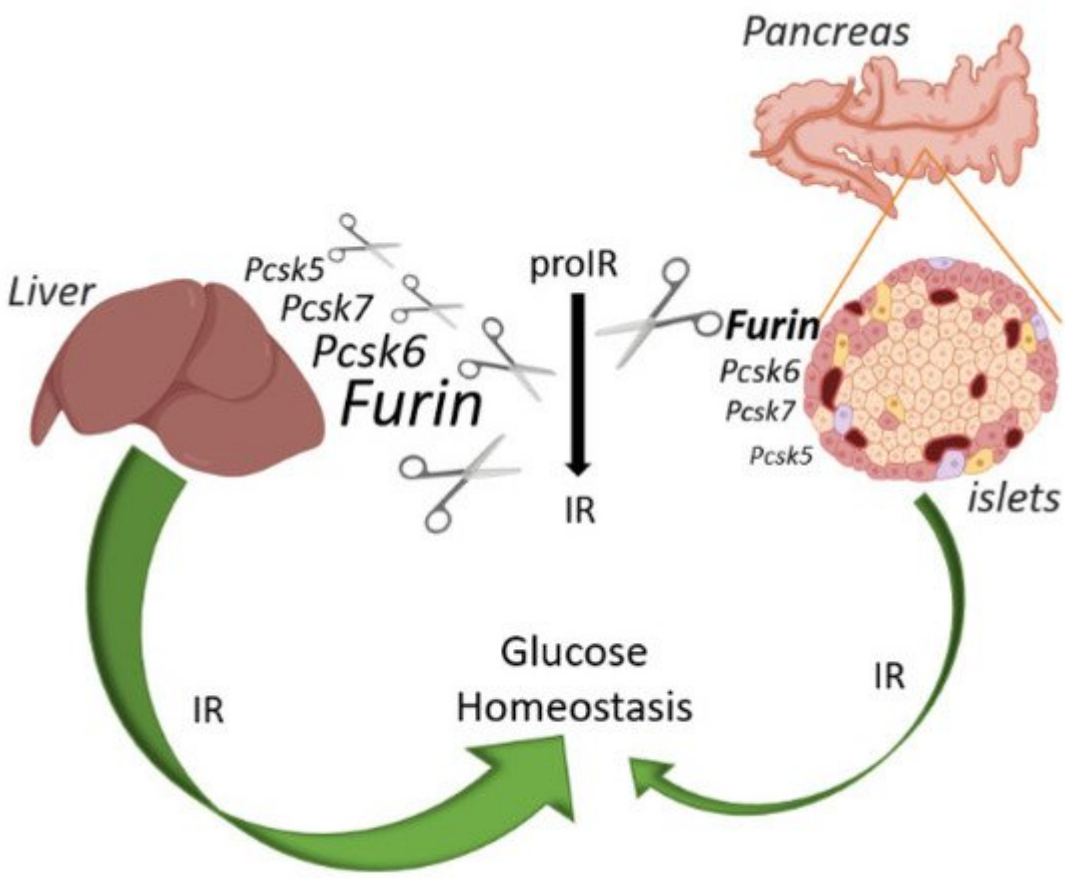

Figure 4. Schematic overview of the IR action on glucose and relative abundance of each PC in liver and pancreatic islets of mice. FURIN non-redundantly cleaves the proIR in pancreatic beta cells of mice, but the IR exerts only a minor effect on glucose homeostasis. In contrast, proprotein convertases other than FURIN can

process proIR in the mouse liver, but here this receptor plays a pivotal role in glucose homeostasis. Image created with BioRender.com.

5. IR Deficiency in Pancreatic β Cells Does Not Induce Severe Glucose Intolerance

IR signaling has distinct roles in liver and pancreas [12][14]. Since the role of the IR in pancreatic β cells is still controversial, we re-evaluated the effect of *Insr* knockout in β cells of mice, using a Cre-driver line without the hGH minigene. We intercrossed RIP-Cre mice [23] with *Insr*-floxed (*Insr*$^{lox/lox}$) animals to generate βIRKO mice (Figure 5A); these mice showed a 68% reduction of *Insr* mRNA in the islets (Figure 5B), consistent with (near) complete inactivation in the β cells. The remaining mRNA expression level was likely linked to the expression of *Insr* in the other cell types of the islets (α, δ cells, and blood vessel endothelial cells), in which the Cre transgene is not expressed. In contrast to earlier observations [13][24], glucose tolerance was not significantly altered in either 12- or 20-week-old mice (Figure 5C–F), and only mildly affected in 24-week-old animals (Figure 5G,H). In addition, fasting blood glucose levels and body weight were unaltered in β*IR*KO mice (Figure S1E,F). Moreover, a previous study reported that *Insr* deficiency in mouse islets and β cell lines led to an induction of ATF4-dependent genes (i.e., Trib3) [25], similar to our previous results using the β*Fur*KO [22]. However, we observed a non-significant reduction in the gene expression levels of *Trib3*, *Chop,* and *Atf4* in isolated islets from the β*IR*KO mice (Figure 5I). This showed that the ATF4 pathway was not altered in these βIRKO mice (Figure 5J).

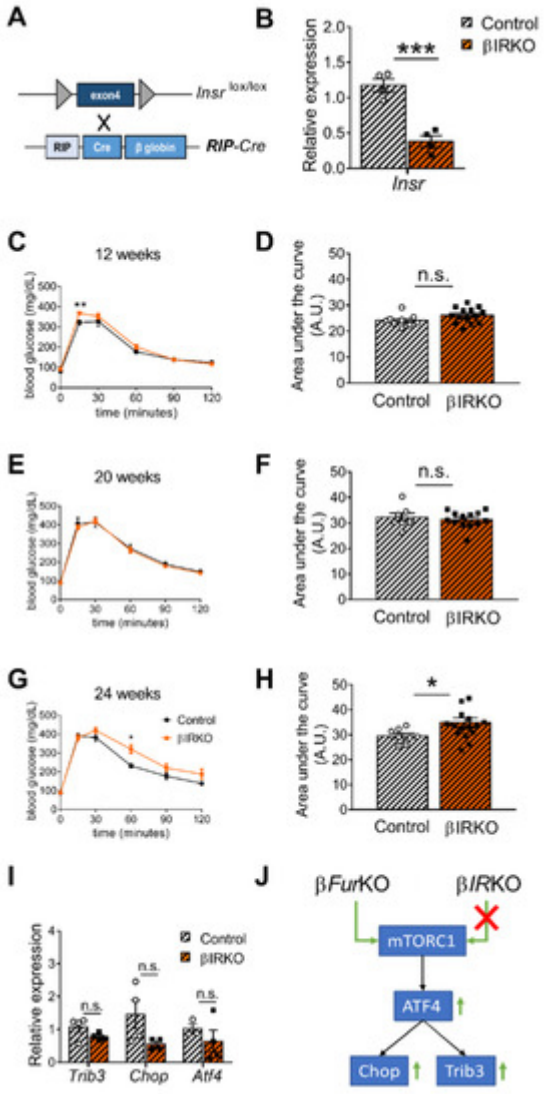

Figure 5. *Insr*-knockout in pancreatic β cells (βIRKO) mildly impairs glucose tolerance in older mice. (**A**) Schematic representation of the breeding approach. Mice expressing the *Insr* gene in which the exon 4 had been floxed (*Insr*$^{lox/lox}$) were crossed with the RIP-Cre driver line. (**B**) RT-qPCR analysis of *Insr* in the islets of control (*Insr*$^{lox/lox}$) and βIRKO mice, *n* = 4 mice/group. All data were normalized to *Gapdh* and to the controls. *** $p < 0.001$ determined by unpaired *t*-test. (**C–H**) IPGTT on male βIRKO and control mice of 12 weeks (*n* = 9–14 mice/group) (**C**), 20 weeks (*n* = 7–13 mice/group) (**E**), and 24 weeks (*n*= 8–16 mice/group) (**G**). Quantification of the area under the curve for (**C**,**E**,**G**) was expressed as g/dL/120 min, and plotted in (**D**,**F**,**H**). * $p < 0.05$, ** $p < 0.01$ determined by two-way ANOVA with a Sidak's multiple comparisons test.* $p < 0.05$ determined by unpaired *t*-test. All data were presented as mean ± SEM. (**I**) RT-qPCR analysis of *Trib3*, *Chop,* and *Atf4* gene expression in the islets of control (*Insr*$^{lox/lox}$) and βIRKO mice, *n* = 3–4 mice/group. No significant differences were detected by two-way ANOVA with Sidak's multiple comparisons test. All the RT-qPCR data were normalized to the *Gapdh*. (**J**) Schematic of mTORC1/ATF4 pathway, which was upregulated in β*Fur*KO but not in βIRKO mice.

References

1. Haeusler, R.A.; McGraw, T.E.; Accili, D. Biochemical and Cellular Properties of Insulin Receptor Signalling. Nat. Rev. Mol. Cell Biol. 2018, 19, 31–44.
2. Bravo, D.A.; Gleason, J.B.; Sanchez, R.I.; Roth, R.A.; Fuller, R.S. Accurate and Efficient Cleavage of the Human Insulin Proreceptor by the Human Proprotein-Processing Protease Furin. Characterization and Kinetic Parameters Using the Purified, Secreted Soluble Protease Expressed by a Recombinant Baculovirus. J. Biol. Chem. 1994, 269, 25830–25837.
3. Yoshimasa, Y.; Seino, S.; Whittaker, J.; Kakehi, T.; Kosaki, A.; Kuzuya, H.; Imura, H.; Bell, G.I.; Steiner, D.F. Insulin-Resistant Diabetes Due to a Point Mutation That Prevents Insulin Proreceptor Processing. Science 1988, 240, 784–787.
4. Kobayashi, M.; Sasaoka, T.; Takata, Y.; Hisatomi, A.; Shigeta, Y. Insulin Resistance by Uncleaved Insulin Proreceptor. Emergence of Binding Site by Trypsin. Diabetes 1988, 37, 653–656.
5. Han, K.; Pierce, S.E.; Li, A.; Spees, K.; Anderson, G.R.; Seoane, J.A.; Lo, Y.-H.; Dubreuil, M.; Olivas, M.; Kamber, R.A.; et al. CRISPR Screens in Cancer Spheroids Identify 3D Growth-Specific Vulnerabilities. Nature 2020, 580, 136–141.
6. Kara, I.; Poggi, M.; Bonardo, B.; Govers, R.; Landrier, J.-F.; Tian, S.; Leibiger, I.; Day, R.; Creemers, J.W.M.; Peiretti, F. The Paired Basic Amino Acid-Cleaving Enzyme 4 (PACE4) Is Involved in the Maturation of Insulin Receptor Isoform B: An Opportunity to Reduce the Specific Insulin Receptor-Dependent Effects of Insulin-like Growth Factor 2 (IGF2). J. Biol. Chem. 2015, 290, 2812–2821.
7. He, Z.; Khatib, A.-M.; Creemers, J.W.M. Loss of Proprotein Convertase Furin in Mammary Gland Impairs ProIGF1R and ProIR Processing and Suppresses Tumorigenesis in Triple Negative Breast Cancer. Cancers 2020, 12, 2686.
8. He, Z.; Thorrez, L.; Siegfried, G.; Meulemans, S.; Evrard, S.; Tejpar, S.; Khatib, A.-M.; Creemers, J.W.M. The Proprotein Convertase Furin Is a Pro-Oncogenic Driver in KRAS and BRAF Driven Colorectal Cancer. Oncogene 2020, 39, 3571–3587.
9. Roebroek, A.J.M.; Taylor, N.A.; Louagie, E.; Pauli, I.; Smeijers, L.; Snellinx, A.; Lauwers, A.; Van de Ven, W.J.M.; Hartmann, D.; Creemers, J.W.M. Limited Redundancy of the Proprotein Convertase Furin in Mouse Liver. J. Biol. Chem. 2004, 279, 53442–53450.
10. Zhang, J.; Liu, F. Tissue-Specific Insulin Signaling in the Regulation of Metabolism and Aging. IUBMB Life 2014, 66, 485–495.
11. Najjar, S.M.; Perdomo, G. Hepatic Insulin Clearance: Mechanism and Physiology. Physiology 2019, 34, 198–215.
12. Michael, M.D.; Kulkarni, R.N.; Postic, C.; Previs, S.F.; Shulman, G.I.; Magnuson, M.A.; Kahn, C.R. Loss of Insulin Signaling in Hepatocytes Leads to Severe Insulin Resistance and Progressive Hepatic Dysfunction. Mol. Cell 2000, 6, 87–97.

13. Kulkarni, R.N.; Brüning, J.C.; Winnay, J.N.; Postic, C.; Magnuson, M.A.; Kahn, C.R. Tissue-Specific Knockout of the Insulin Receptor in Pancreatic Beta Cells Creates an Insulin Secretory Defect Similar to That in Type 2 Diabetes. Cell 1999, 96, 329–339.
14. Okada, T.; Liew, C.W.; Hu, J.; Hinault, C.; Michael, M.D.; Krtzfeldt, J.; Yin, C.; Holzenberger, M.; Stoffel, M.; Kulkarni, R.N. Insulin Receptors in Beta-Cells Are Critical for Islet Compensatory Growth Response to Insulin Resistance. Proc. Natl. Acad. Sci. USA 2007, 104, 8977–8982.
15. Otani, K.; Kulkarni, R.N.; Baldwin, A.C.; Krutzfeldt, J.; Ueki, K.; Stoffel, M.; Kahn, C.R.; Polonsky, K.S. Reduced Beta-Cell Mass and Altered Glucose Sensing Impair Insulin-Secretory Function in BetaIRKO Mice. Am. J. Physiol. Endocrinol. Metab. 2004, 286, E41–E49.
16. Wicksteed, B.; Brissova, M.; Yan, W.; Opland, D.M.; Plank, J.L.; Reinert, R.B.; Dickson, L.M.; Tamarina, N.A.; Philipson, L.H.; Shostak, A.; et al. Conditional Gene Targeting in Mouse Pancreatic SS-Cells: Analysis of Ectopic Cre Transgene Expression in the Brain. Diabetes 2010, 59, 3090–3098.
17. Brouwers, B.; de Faudeur, G.; Osipovich, A.B.; Goyvaerts, L.; Lemaire, K.; Boesmans, L.; Cauwelier, E.J.G.; Granvik, M.; Pruniau, V.P.E.G.; Van Lommel, L.; et al. Impaired Islet Function in Commonly Used Transgenic Mouse Lines Due to Human Growth Hormone Minigene Expression. Cell Metab. 2014, 20, 979–990.
18. Transgenic Artifacts Caused by Passenger Human Growth Hormone. Abstract—Europe PMC. Available online: (accessed on 27 October 2020).
19. Oropeza, D.; Jouvet, N.; Budry, L.; Campbell, J.E.; Bouyakdan, K.; Lacombe, J.; Perron, G.; Bergeron, V.; Neuman, J.C.; Brar, H.K.; et al. Phenotypic Characterization of MIP-CreERT1Lphi Mice with Transgene-Driven Islet Expression of Human Growth Hormone. Diabetes 2015, 64, 3798–3807.
20. Oakie, A.; Zhou, L.; Rivers, S.; Cheung, C.; Li, J.; Wang, R. Postnatal Knockout of Beta Cell Insulin Receptor Impaired Insulin Secretion in Male Mice Exposed to High-Fat Diet Stress. Mol. Cell Endocrinol. 2020, 499, 110588.
21. Skovsø, S.; Panzhinskiy, E.; Kolic, J.; Dionne, D.A.; Dai, X.-Q.; Sharma, R.B.; Elghazi, L.; Cen, H.H.; Ellis, C.E.; Faulkner, K.; et al. Beta-Cell specific insulin resistance promotes glucose-stimulated insulin hypersecretion. bioRxiv 2020.
22. Brouwers, B.; Coppola, I.; Vints, K.; Dislich, B.; Jouvet, N.; Lommel, L.V.; Segers, C.; Gounko, N.V.; Thorrez, L.; Schuit, F.; et al. Loss of furin in β Cells induces an MTORC1-ATF4 anabolic pathway that leads to β cell dysfunction. Diabetes 2020.
23. Herrera, P.L. Adult insulin- and glucagon-producing cells differentiate from two independent cell lineages. Development 2000, 127, 2317–2322.

24. Postic, C.; Shiota, M.; Niswender, K.D.; Jetton, T.L.; Chen, Y.; Moates, J.M.; Shelton, K.D.; Lindner, J.; Cherrington, A.D.; Magnuson, M.A. Dual roles for glucokinase in glucose homeostasis as determined by liver and pancreatic beta cell-specific gene knock-outs using cre recombinase. J. Biol. Chem. 1999, 274, 305–315.
25. Liew, C.W.; Bochenski, J.; Kawamori, D.; Hu, J.; Leech, C.A.; Wanic, K.; Malecki, M.; Warram, J.H.; Qi, L.; Krolewski, A.S.; et al. The pseudokinase tribbles homolog 3 interacts with atf4 to negatively regulate insulin exocytosis in human and mouse β cells. J. Clin. Investig. 2010, 120, 2876–2888.